

Computer simulation calculations of the free liquid surface of mercury

J.-M. Bomont* and J.-L. Bretonnet

Laboratoire de Physique des Milieux Denses, Université Paul Verlaine, 57078 Metz, France

D. J. Gonzalez and L. E. Gonzalez

Departamento de Física Teórica, Universidad de Valladolid, 47011 Valladolid, Spain

(Received 27 January 2009; published 8 April 2009)

Oscillatory density profiles are a well-known feature occurring at the free surfaces of liquid metals. Recently, the thermophysical properties of expanded liquid mercury have been successfully investigated with an atypical isotropic effective interaction [Bomont *et al.*, *J. Chem. Phys.* **124**, 054504 (2006)]. We use this model to investigate the liquid-vapor interface properties taking explicitly into account the density dependence of the potential related to the metal-nonmetal transition along the interface. Ionic and electronic density distributions along the normal of the interface display strong stratification and the calculated reflectivities compare well with experimental data.

DOI: [10.1103/PhysRevB.79.144202](https://doi.org/10.1103/PhysRevB.79.144202)

PACS number(s): 61.20.Ja, 61.20.Lc, 61.25.Mv, 71.15.Pd

It had long been believed that, at the free liquid surface, the surface-normal (longitudinal) density profile (DP) decreased monotonically from the bulk liquid density to that of the vapor.¹ However, in 1973, theoretical results of Rice *et al.*² revealed considerable structure at liquid metal surfaces in the form of stable ionic density oscillations. This is the surface-induced layering phenomenon, whereby the liquid atoms or ions arrange themselves into layers parallel to the surface across the interfacial transition zone. The density oscillations were found to be quite strong, with peak values in the layers larger than the bulk liquid density. A substantial amount of theoretical work has followed,^{3,4} with the goal of understanding how surface-induced layering depends on the interactions between atoms. In 1995, x-ray scattering experiments probed the existence of such order near the surfaces of a number of liquid metals.⁵ The characteristic signature of surface layering in experiments is a strong peak in the x-ray reflectivity intensity at large values of the wave-vector transfer q_z . Contrary to liquid metals, no evidence of such phenomenon was found for classical dielectric liquids.⁶⁻⁹ This difference was first attributed to the fact that the surface tension γ of most liquid metals is high (≈ 500 mN/m) so that their surface is very smooth, while dielectric liquids have much smaller surface tension (frequently lower than 40 mN/m) and therefore have much rougher surfaces to exhibit layers.¹⁰ However, even if water¹¹ and potassium¹² have comparable surface tensions, no evidence for layering has been shown for the former, and this showed that more than pure surface-tension effects are needed to account for the layering mechanism. The obvious feature that distinguishes metals from dielectrics is the presence of an electron gas. Moreover, in a metal the nature of the interactions changes markedly across the interface: the bonding changes from metallic (with delocalized valence electrons in the bulk liquid) to van der Waals type (with localized electrons on the atoms in the vapor), leading to a metal-nonmetal (M-NM) transition. Theoretical works, based on simulations, have resulted in a number of hypotheses for the mechanism of surface-induced layering. One of them¹³ suggested that it would be caused by geometrical confinement effects, by analogy with the known phenomenon that layers form in the liquid (me-

talic or not) near a solid-liquid interface. In this way, the rapid decay of the valence electronic density would induce a flat high-tension surface acting as a hard wall against which the atoms are packed. Another suggestion¹⁴ stated that the undercoordinated atoms near the surface attempt to regain the favorable coordination they would have in the bulk liquid, resulting in an increased density in the outermost liquid part and causing the propagation of a density oscillation into the bulk part. As a consequence, layering has been believed to be absent at the liquid surface of simple fluids with isotropic interactions and was thought to be unique to metallic liquids. This last statement has been however called into question by several recent works. In particular, Chacon *et al.*¹⁵ hinted that metallic bonding would not play such a crucial role in the formation of layers at the free metallic surfaces. Many liquid metals are characterized by a high critical temperature T_C and a low melting temperature T_M . For example, layering is observed in mercury at room temperature ($T=0.15T_C$, while $T_M/T_C=0.13$). By using classical simulations, the authors found out that (i) a low freezing point and high critical point can be produced by a broad and shallow pair potential and (ii) that an oscillating ionic DP should appear at the free liquid surface of any substance (metallic or not), provided that it has a low T_M/T_C ratio. The appearance of oscillating profiles for this type of potentials was confirmed by Li and Rice,¹⁶ who termed these systems “Madrid liquids” (ML). However the density oscillations do not resemble those obtained for metallic systems, showing peak values in the layers smaller than the bulk density. Recent *ab initio* simulation results for sodium¹⁷ provide some support to the finding of Chacon *et al.*¹⁵ by concluding that neither Friedel oscillations nor rearrangements induced by undercoordinated atoms have any effects on the surface layering. Furthermore, Chacon *et al.* arguments¹⁸ was supported by a recent x-ray reflectivity experiment where surface layering was observed in a molecular nonliquid-crystalline nonmetallic liquid, with a low melting point and a high critical point.

These recent advances imply that some of the conventional arguments concerning our understanding of the surface-induced layering phenomenon must be re-examined after pausing and listing some questions that a satisfactory

theory should explain. The main questions concern the nature itself of layering. Is it a universal property of liquids at low enough temperature? If so, would it be possible to predict qualitatively and quantitatively the main features of x-ray reflectivity measurements by using a simplified formalism? And more specifically, which are the essential features that the potential must have in order to obtain a strongly oscillating DP? To answer these questions, we pursue the idea of presenting a very simplified and comprehensive description of the liquid-vapor (LV) interface which we apply to liquid mercury (l-Hg).

A distinctive feature of l-Hg is that the M-NM transition does not occur at the liquid-vapor critical density ($\rho_C = 5.3 \text{ g/cm}^3$) but rather gradually, in the range from $\rho_1 = 11 \text{ g/cm}^3$ to $\rho_2 = 8 \text{ g/cm}^3$. This means that the M-NM transition occurs across the interface, making its study a difficult and challenging problem. Indeed, we are aware of only two previous theoretical studies¹⁹ based on MC simulations involving pseudopotential formalism, which were performed long before the previously mentioned advances. To date, the x-ray reflectivity data for l-Hg at both melting and room temperatures²⁰ have not yet been reproduced by any theoretical calculation including classical or *ab initio* simulations. A main reason is that most of existing pair interaction models overestimate the melting temperature of real systems. Thus the observation of the oscillatory DP at the free liquid surface is very often pre-empted by solidification. For the present investigation, we have used an interaction model, developed in a previous work²¹ for studying the static bulk properties of l-Hg. This model has already shown its capability to properly predict the liquid branch of the coexistence L/V phase diagram in terms of temperature and density (implying that it effectively incorporates subtle many-body effects). The potential is of the ML type, reading

$$\Phi(r_{ij}) = A_0 \exp(-\alpha r_{ij}) - A_1 \exp[-\beta(r_{ij} - R_0)^2], \quad (1)$$

and, contrary to pseudopotential theory, does not exhibit long-range Friedel oscillations. Excepting A_1 which satisfies an empirical law, the four remaining parameters remain constant along the whole LV coexistence curve. Additional details are given in Ref. 21. Computer simulations of the LV interface with this potential, as such, have yielded typical ML DPs, i.e., oscillating but not strongly.²² In this work we allow the potential to incorporate the effects of the attendant M-NM transition that occurs in the interface by allowing the parameter A_1 change according to the character of the atoms. The character of an atom labeled as i is defined on the basis of its local reference density $\rho_i = \rho(\mathbf{R}_i)$, which varies from a configuration to another. Using Rice's ideas,¹⁹ we use a "metallic character" function $f(\rho)$ that is 1 for $\rho \geq \rho_1$, 0 for $\rho \leq \rho_2$, and varies smoothly in between. Therefore an atom i is considered as metallic (M) when $f_i = f(\rho_i)$ is equal to one, vaporized (V) when $f_i = 0$ and in a "hybrid state" (i.e., neither metallic nor vaporized) when $0 < f_i < 1$. In their work, Rice *et al.*¹⁹ defined the metal-metal (MM) potential from the pseudopotential formalism and the metal-vapor (MV) potential in the same Born-Mayer analytical form as the vapor-vapor (VV) potential. Previously, Evans²³ proposed that the interactions between pairs of atoms of identical character

should be written in the same form. Following Evans' suggestion, we assume the unique form of Eq. (1) for the three types of interactions and postulate that the value of A_1 for the interaction between atoms i and j is

$$A_1 = f_i f_j A_1^{\text{MM}} + [f_i(1 - f_j) + (1 - f_i)f_j] A_1^{\text{MV}} + (1 - f_i)(1 - f_j) A_1^{\text{VV}}. \quad (2)$$

This methodology can describe equally well bulk (metallic) and surface (hybrid or vaporized) atoms. Note that previous studies^{15,22} used $f_i = f_j = 1$ (or alternatively $A_1^{\text{MV}} = A_1^{\text{VV}} = A_1^{\text{MM}}$), leading to $A_1 = A_1^{\text{MM}}$ for all pairs of particles and to oscillatory but non-typical-metallic profiles. The atoms move during the simulation and consequently $\rho(\mathbf{R}_i)$ varies with the evolving local environment, which in turn implies a variation in the character of the atoms with respective positions. Therefore, in order to perform a suitable average over all atomic configurations, the pair interactions have to be *de facto* calculated in a self-consistent manner through Eq. (2). To simulate the interface, we performed self-consistent simulations without applying periodic boundary conditions along the z axis but only along the x and y axes, for which we used a box with $L_x = L_y = 24.56 \text{ \AA}$. We considered 864 particles, and it is important to remark that the bulk density ρ_b obtained as a result of the simulation of the interface reproduces correctly the experimental one. The number of atoms in the interface is a small fraction (3%–4%) of the total number of atoms so that changes in the interface's structure do not affect the atomic density distribution in the bulk liquid. In the present calculation, the interfaces are allowed to relax for 2 ns and properties of interest are averaged over another run of 6 ns.

In the usual analysis of the experimental results, the ionic DPs are "reverse engineered" by fitting the obtained x-ray reflectivity intensity data to some mathematical model of the DP. In fact, the experimental analysis of the free liquid surface probes the longitudinal total electronic density distribution. The reflected intensity $R(q_z)$ is

$$R(q_z)/R_F(q_z) = |\Phi_{\text{int}}(q_z)|^2 \exp(-\sigma_c^2 q_z^2), \quad (3)$$

where q_z is the momentum transfer perpendicular to the interface, $R_F(q_z)$ is the Fresnel reflectivity of a perfectly sharp step-function interface, and $\Phi_{\text{int}}(q_z)$ is the intrinsic surface structure factor,

$$\Phi_{\text{int}}(q_z) = \frac{1}{\rho_{e,B}^T} \int_{-\infty}^{\infty} \left(\frac{\partial \rho_{e,\text{int}}^T(z)}{\partial z} \right) \exp(iq_z z) dz, \quad (4)$$

where $\rho_{e,B}^T$ is the bulk total electron density and $\rho_{e,\text{int}}^T(z)$ is the intrinsic (i.e., in the absence of capillary-wave smearing) longitudinal electronic DP. The term $\exp(-\sigma_c^2 q_z^2)$ in Eq. (3) accounts for the effects on $R(q_z)$ of the thermally induced surface roughness, with $\sigma_c^2 = \sigma_0^2 + \sigma_{\text{cw}}^2$, where σ_0 is an intrinsic roughness and σ_{cw} accounts for the capillary waves.^{3,4}

In the simulations, we proceed in the opposite way to the experimental analysis since we obtain the time-averaged longitudinal total electronic DPs $\rho_e^T(z)$, through the superposi-

TABLE I. Parameters relative to our self-consistent molecular-dynamics calculations.

| T (K) | A_1^{MM} (eV) ^a | A_1^{MV} (eV) | $\sigma_{\text{cw}}^{\text{expt.}}$ (Å) ^b | $\sigma_{\text{cw}}^{\text{th}}$ (Å) |
|---------|-------------------------------------|------------------------|--|--------------------------------------|
| 235 | 0.0381 | 0.122 | 0.726 | 0.467 |
| 293 | 0.0421 | 0.0842 | 0.820 | 0.529 |

^aFrom Ref. 21.

^bFrom Ref. 20.

tion of atomic electron densities on each of the ionic positions.²⁴ These DPs already include some thermal fluctuations and give a reflected intensity,

$$\frac{R(q_z)}{R_F(q_z)} = \left| \frac{1}{\rho_{e0}} \int_{-\infty}^{\infty} \left(\frac{\partial \rho_e^T(z)}{\partial z} \right) \exp(iq_z z) dz \right|^2 \equiv |\Phi(q_z)|^2. \quad (5)$$

Notice that the simulated surface structure factor $\Phi(q_z)$ appears as the convolution of the intrinsic one, $\Phi_{\text{int}}(q_z)$, with an associated Gaussian distribution describing the simulation's capillary waves. These latter ones are described by the term $\sigma_{\text{cw}}^{\text{th}}$ whose value depends on the temperature and the interface's area. Given the greater interface's area of the experimental sample, the associated $\sigma_{\text{cw}}^{\text{expt.}}$ differs from the simulation's one (indeed, $\sigma_{\text{cw}}^{\text{expt.}} > \sigma_{\text{cw}}^{\text{th}}$) and a proper comparison between the theoretical and experimental reflectivities requires inclusion of the same range of capillary waves in both calculations. This is achieved by computing the simulation reflectivity⁴ as

$$R(q_z)/R_F(q_z) = |\Phi(q_z)|^2 \exp[-(\Delta\sigma_{\text{cw}}^2 + \sigma_0^2)q_z^2],$$

where $\Delta\sigma_{\text{cw}}^2 = (\sigma_{\text{cw}}^{\text{expt.}})^2 - (\sigma_{\text{cw}}^{\text{th}})^2$. Unfortunately, σ_0 has not a clear physical meaning although it has been related to atomic size. However, it is an important input in those (nonunique) mathematical models used in the fitting of experimental data. Moreover, for l-Hg, σ_0 was first assumed⁵ to be a constant but it was later found²⁰ that a temperature dependence produced better fits to the experimental data. In this work we have decided to discard this controversial contribution because it does not alter the conclusions obtained.

To perform our self-consistent DPs calculations, we *a priori* have to deal with two free parameters A_1^{MV} and A_1^{VV} , since A_1^{MM} is already known²¹ at each temperature. Their values have been determined so that the corresponding electronic DP $\rho_e^T(z)$ provides the best agreement with the experimental reflectivity. In these calculations, we found that for a given A_1^{MV} the values of A_1^{VV} had a negligible influence on the DPs. This is not surprising, since it reflects that the "floating" vapor ($\rho_v \sim 10^{-5}\rho_b$) above the liquid does not influence the interface and/or bulk structures. Consequently, our approach reduces to fixing the parameter A_1^{MV} , whose values are shown in Table I. As can be seen, A_1^{MV} is systematically larger than A_1^{MM} , suggesting that more attraction is needed at the interface than in the bulk.

Normalized longitudinal atomic and electronic DPs calculated from self-consistent molecular dynamics appear in Fig. 1. There are marked oscillations in the atomic DPs indicating

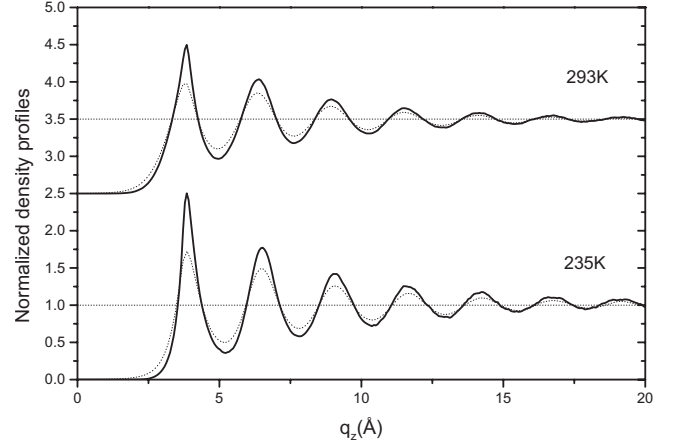


FIG. 1. Normalized ionic (solid lines) and electronic (dotted lines) DP at melting and room temperatures. For sake of clarity, room-temperature results have been shifted by 2.5.

the existence of layers at the interface. The electronic DPs follow the atomic ones albeit with weaker oscillations. These are stronger at melting than at room temperature, which is expected as thermal effects tending to smear out the layering structure with increasing temperature. Moreover at room temperature the ratio $A_1^{\text{MV}}/A_1^{\text{MM}}$ is lower than the one at melting. This conspires with the increased thermal roughness to produce a less structured interface. The ratio between the peak density of the layers and the bulk density is found to be larger than one at each temperature. So, the final calculated longitudinal DPs do exhibit the basic features that are expected in liquid metals.

In Fig. 2 we depict the corresponding reflectivities which closely agree with their experimental counterparts²⁰ at both temperatures. The surface-induced layering is strongly temperature dependent: at the melting point, the quasi-Bragg peak has a large amplitude, while at room temperature it is less pronounced. Squared moduli of the surface structure factors present a clear maximum with expected intensity even if the location overestimates slightly the one provided by experiment. We attribute this discrepancy to small inaccuracies

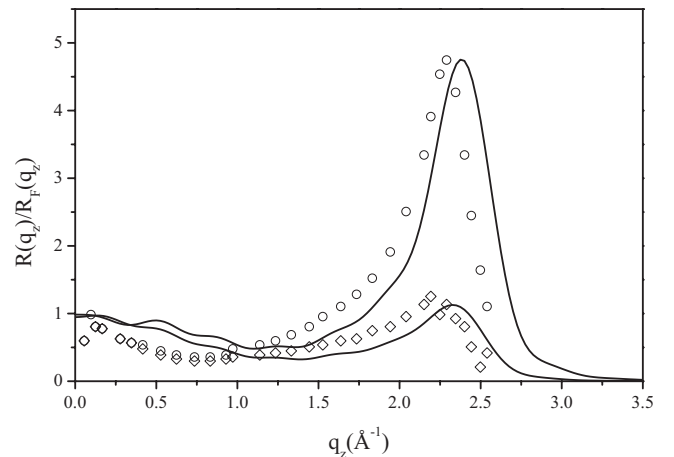


FIG. 2. Calculated reflectivities at melting and room temperatures (from top to bottom)

in our simple model. Nevertheless, a minimum at low-momentum transfer wave vector is distinguishable as observed in experimental data for l-Hg (not for Ga), while the ripples are a known artifact from the limited simulation cell size.

From the comparison among the standard approach to liquid metals,¹⁹ the standard ML approach^{15,16,22} and the one proposed here we can deduce which characteristics of the former (Friedel oscillations in the potential, density-dependent and structure-independent terms in the energy and density dependences of the interactions) are essential to obtain strongly oscillating DPs that lead to clear peaks in the reflectivity. While ML lead to oscillatory DPs, it is only when the potential is allowed to change with density that typical metallic results are found.

In summary, we have shown that the main features of x-ray reflectivity measurements at the free liquid surface of Hg can be qualitatively and quantitatively predicted by using an extremely simplified approach. The predominant interac-

tions (through A_1^{MV}) near the surface, and in particular their variation with density, have been shown to be, in our case, the driving force in the strong layering mechanism. Since similar results can be obtained with both pseudopotentials and ML formalisms, we conclude that surface-induced layering is a universal property of liquids at low enough temperatures provided that (i) they have a low T_M/T_C ratio and (ii) the potential changes along the liquid-vapor interface, either in form (pseudopotentials) or in magnitude (ML). The present theoretical study may encourage new experiments for nonmetallic liquids that could reveal unsuspected and interesting properties of matter for scientific applications.

The Pôle Messin de Simulation is gratefully acknowledged for providing us with computer time. Thanks to E. Gallant for technical support. D.J.G. and L.E.G. acknowledge support from MCINN (under Contract No. FIS2008-02490/FIS), JCyL (under Contract No. VA068A06, GR120), and the EU FEDER program.

*Corresponding author. bomont@univ-metz.fr

¹J. S. Rowlinson and B. Widom, *Molecular Theory of Capillarity* (Oxford University Press, New York, 1982).

²S. A. Rice, D. Guidotti, H. L. Lemberg, W. C. Murphy, and A. N. Bloch, in *Advances in Chemical Physics XXVII*, edited by I. R. Priogogine and S. A. Rice (Wiley, New York, 1974).

³J. Penfold, *Rep. Prog. Phys.* **64**, 777 (2001); S. A. Rice, *Mol. Simul.* **29**, 593 (2003).

⁴L. E. Gonzalez and D. J. Gonzalez, *Phys. Rev. B* **77**, 064202 (2008).

⁵O. M. Magnussen, B. M. Ocko, M. J. Regan, K. Penanen, P. S. Pershan, and M. Deutsch, *Phys. Rev. Lett.* **74**, 4444 (1995); M. J. Regan, E. H. Kawamoto, S. Lee, P. S. Pershan, N. Maskil, M. Deutsch, O. M. Magnussen, B. M. Ocko, and L. E. Berman, *ibid.* **75**, 2498 (1995); H. Tostmann, E. DiMasi, P. S. Pershan, B. M. Ocko, O. G. Shpyrko, and M. Deutsch, *Phys. Rev. B* **59**, 783 (1999).

⁶A. Braslau, M. Deutsch, P. S. Pershan, A. H. Weiss, J. Als-Nielsen, and J. Bohr, *Phys. Rev. Lett.* **54**, 114 (1985).

⁷M. K. Sanyal, S. K. Sinha, K. G. Huang, and B. M. Ocko, *Phys. Rev. Lett.* **66**, 628 (1991).

⁸W. Zhao, X. Zhao, J. Sokolov, M. H. Rafailovich, M. K. Sanyal, S. K. Sinha, and B. H. Cao, *J. Chem. Phys.* **97**, 8536 (1992); W. Zhao, M. H. Rafailovich, J. Sokolov, L. J. Fetters, R. Plano, M. K. Sanyal, S. K. Sinha, and B. B. Sauer, *Phys. Rev. Lett.* **70**, 1453 (1993).

⁹B. M. Ocko, X. Z. Wu, E. B. Sirota, S. K. Sinha, and M. Deutsch, *Phys. Rev. Lett.* **72**, 242 (1994).

¹⁰J. M. Soler, G. Fabricius, and E. Artacho, *Surf. Sci.* **482-485**, 1314 (2001).

¹¹O. Shpyrko, M. Fukuto, P. Pershan, B. Ocko, I. Kuzmenko, T. Gog, and M. Deutsch, *Phys. Rev. B* **69**, 245423 (2004).

¹²C. J. Yu, A. G. Richter, A. Datta, M. K. Durbin, and P. Dutta, *Phys. Rev. Lett.* **82**, 2326 (1999).

¹³J. G. Harris, J. Gryko, and S. A. Rice, *J. Chem. Phys.* **87**, 3069 (1987); *J. Stat. Phys.* **48**, 1109 (1987).

¹⁴S. Iarlori, P. Carnevali, F. Ercolessi, and E. Tosatti, *Surf. Sci.* **211-212**, 55 (1989); F. D. Ditolla, Ph.D. thesis, SISSA, 1996.

¹⁵E. Chacon, M. Reinaldo-Falagan, E. Velasco, and P. Tarazona, *Phys. Rev. Lett.* **87**, 166101 (2001); P. Tarazona, E. Chacon, and M. Renaldo-Falagan, *J. Chem. Phys.* **117**, 3941 (2002); E. Velasco, P. Tarazona, M. Renaldo-Falagan, and E. Chacon, *ibid.* **117**, 10777 (2002).

¹⁶D. Li and S. A. Rice, *J. Phys. Chem. B* **108**, 19640 (2004).

¹⁷B. G. Walker, N. Marzari, and C. Molteni, *J. Chem. Phys.* **124**, 174702 (2006).

¹⁸H. Mo, G. Evmenenko, S. Kewalramani, K. Kim, S. N. Ehrlich, and P. Dutta, *Phys. Rev. Lett.* **96**, 096107 (2006).

¹⁹M. P. D'Evelyn and S. A. Rice, *J. Chem. Phys.* **78**, 5081 (1983); D. S. Chekmarev, M. Zhao, and S. A. Rice, *Phys. Rev. E* **59**, 479 (1999).

²⁰E. DiMasi, H. Tostmann, B. M. Ocko, P. S. Pershan, M. Deutsch, *Phys. Rev. B* **58**, R13419 (1998).

²¹J. M. Bomont and J. L. Bretonnet, *J. Chem. Phys.* **124**, 054504 (2006).

²²J. M. Bomont and J. L. Bretonnet, *J. Phys.: Conf. Ser.* **98**, 042018 (2008).

²³R. Evans, *J. Phys. C* **7**, 2808 (1974).

²⁴Although it may be argued that the valence electronic density changes from the free atom to the present slab, this has no practical consequences on $\rho_e^T(z)$ because the main contribution comes from the core electrons whose distribution remains practically unchanged.